Locus-specific chromatin proteomics using dCas-guided proximity labelling in *Aspergillus nidulans.*

Thomas Svoboda[1*], Dominik Niederdöckl-Loibl[1*], Andreas Schüller[1], Karin Hummel[2], Sarah Schlosser[2], Ebrahim Razzazi-Fazeli[2], and Joseph Strauss[1+]

[*] These authors contributed equally

[+] corresponding author

[1] Institute of Microbial Genetics, Department of Applied Genetics and Cell Biology, BOKU University Vienna, Campus Tulln, Konrad Lorenz Strasse 24, 3430, Tulln an der Donau, Austria.

[2] VetCore Facility, University of Veterinary Medicine, Veterinärplatz 1, 1210 Vienna, Austria.

Abstract

Proximity labelling that uses promiscuous biotin ligases (BirA) fused to a bait protein is a powerful tool to identify protein interaction partners *in vivo* under different metabolic or developmental conditions. BirA can also be used to determine protein composition and interaction partners at specific chromatin locations when it is fused with enzymatically-disabled Cas9 (dCas9) and then guided to the location of interest by sgRNAs. We adapted this method (called CasID) for fungal cells using the nitrate assimilation gene cluster of *A. nidulans* as a model locus and estrogen-inducible expression of the dCas9-BirA fusion to improve condition-specific labelling. For method establishment, we first verified the presence of dCas-BirA and a known transcription factor at the nitrate locus by chromatin immunoprecipitation (ChIP). Results show that both dCas-BirA and the AreA transcription factor are present at the locus of interest under the conditions used for biotinylation. We then optimized the CasID procedure for efficient labelling and background reduction using the CasID-sgRNA strain and two control strains, one lacking the sgRNA and another one lacking the whole CasID system. Here we provide proof-of-concept for the suitability of the method by showing that biotinylated proteins are enriched in the CasID strains in comparison to the controls. After background reduction, 32 proteins remained in two independent experiments exclusively enriched in the Cas-ID-sgRNA strain. Among these proteins was NmrA, an AreA-interacting regulator, and we also found several chromatin-associated proteins. Overall, our results demonstrate that Cas-ID is suitable for locus-specific labelling and identification of chromatin-associated proteins and transcription factors in *A. nidulans*. However, the high background of proteins that are biotinylated out of chromatin context or unspecifically attach to the affinity purification matrix needs to be addressed by implementing a set of rigorous controls. In summary, we herewith provide a detailed protocol for application of the method that proved to be useful for the identification of novel chromatin-associated proteins and their interaction partners at a specific genomic locus in divers metabolic and developmental conditions.

Author summary

This study demonstrates that locus-specific proteomics can be carried out by dCas-BirA guided proximity labelling in *Aspergillus nidulans.* For establishment, we targeted the well-described bidirectional promoter region between *niaD*, a nitrate reductase, and *niiA*, a nitrite reductase. At this locus we could test by chromatin immunoprecipitation (ChIP) in combination with qPCR if both, the dCas9-BirA fusion as well as a central transcription factor are at the locus under the conditions of our Cas-ID experiment. After this first control step, we considered that unspecific labelling by dCas-BirA during the time from translation to landing at the targeted chromatin locus may be one of the most relevant drawbacks of the method. Therefore, we developed a number of control strains that would allow us to clearly discriminate between background and sgRNA-dependent specific labelling at the locus. Our protein MS results validated these estimates and only considering the results of these controls enabled us to distinguish the set of locus-specific proteins from a very high general background. Finally, enrichment of biotinylated proteins through affinity purification with streptavidin resin and subsequent LC-MS/MS analysis showed that more than 800 proteins were detected in each sample, emphasizing the high background of the purification method. After background reduction of the control samples, we were able to identify 32 proteins which were exclusively detected in the test strain in two independent measurements, including several chromatin-associated proteins and NmrA, a negative regulator of the nitrate locus transcription factor AreA.

Introduction

Proximity-dependent labelling is a molecular tool to assess interaction partners of proteins in living cells and is frequently used as an alternative to co-immunoprecipitation (co-IP) or other affinity-tag based enrichment techniques for protein complexes. The advantage of proximity labelling over the other techniques is that it also detects weak or only transient interactions and the method has been developed and optimized over the last decade (reviewed by Samavarchi-Tehrani et al., 2020). The most

61 commonly used labelling molecule is biotin and there are biotin ligases as well as peroxidases available
62 for biotinylation approaches. While HRP or APEX require biotin-phenol as well as peroxide as substrate
63 and attach it to tyrosine, the promiscuous biotin ligase BirA (or an engineered version of it named
64 TurboID), uses biotin as substrate and attaches the activated biotinyl-5´-AMP to lysine residues. Also
65 different other versions like mini TurboID are available (reviewed by Samavarchi-Tehrani et al., 2020).
66 Proximity labelling employing BirA or derivatives of it has already been used in many different
67 organisms ranging from mammalian cells (Cho et al., 2020), Zebrafish (Xiong et al., 2021), different
68 plant species (Yang et al., 2021) to yeast (Singer-Krüger and Jansen, 2022) and recently also to
69 *Aspergillus nidulans* (Georgiou et al., 2023).

70 Beside fusing the biotin ligase to a bait-protein for which the interaction partner(s) should be
71 identified, also fusion to enzymatically disabled "dead" Cas9 (dCas) is possible. dCas is still able to
72 interact with single guide RNAs (sgRNAs) and bind the target location in DNA, however, due to a
73 specific mutation, it cannot cut the DNA anymore. This allows the construction of a fused dCas-BirA
74 chimera that produces a biotinyl-5´-AMP cloud at the target chromosomal location thereby
75 biotinylating proteins that are in close proximity within a radius of approximately 30nm. dCas can be
76 guided to a defined locus at the DNA by a designed sgRNA. This method thus allows locus-specific
77 proteomics through the guidance of the proximity labelling system to a specific genomic locus in the
78 living cell and to assess there the chromatin composition under defined experimental conditions
79 (reviewed by Anton et al., 2018).

80 In this study we established the CasID protocol expressing TurboID-dCas and sgRNAs in *Aspergillus*
81 *nidulans* which genome consists of 8 chromosomes encoding approximately 12.000 genes. One of the
82 first metabolic pathways that were studied on a detailed genetic and molecular level using this model
83 fungus was nitrate assimilation. In bacteria, fungi and plants this pathway allows to use oxidized nitrate
84 as nitrogen source for growth and to reduce it to ammonium for the further incorporation into amino
85 acids (Cove, 1979). A wealth of knowledge is available on the *cis*-acting regions and *trans*-acting factors
86 regulating transcription of the genes involved in nitrate assimilation (Burger et al., 1991; Gallmetzer et

87 al., 2015; Muro-Pastor et al., 1999; Punt et al., 1995; Scazzocchio, 2000; Scazzocchio and Arst, 1989;
88 Schinko et al., 2010; Strauss et al., 1998). The genes are induced by the nitrate-specific C_6Zn_2-family
89 transcription factor NirA that interacts with the GATA-type transcriptional activator AreA and together
90 they synergistically activate their target genes (Berger et al., 2008; Berger et al., 2006; Kudla et al.,
91 1990). Under nitrate-inducing conditions, NirA switches conformation, accumulates in the nucleus and
92 both regulators bind to the promoter regions of nitrate-responsive genes (Bernreiter et al., 2007;
93 Gallmetzer et al., 2015). AreA recruits histone acetylation to chromatin (Muro-Pastor et al., 1999;
94 Muro-Pastor et al., 2004) and activates transcription synergistically with NirA. To prevent waste of
95 energy, AreA is inactivated when the intracellular levels of already reduced nitrogen sources such as
96 ammonium or glutamine are already high. Previous binding experiments using *in vivo* footprinting
97 (Muro-Pastor et al., 1999; Muro-Pastor et al., 2004) or ChIP of an HA-AreA strain (Berger et al., 2008;
98 Berger et al., 2006) demonstrated that binding of AreA is lost upon repression by ammonium. The
99 mechanism behind AreA inactivation has been studied in detail and was found to be modulated by
100 NmrA, a regulatory protein able to monitor the nitrogen status of the cell and eventually block AreA
101 activity when reduced nitrogen levels are high (Lamb et al., 2003; Langdon et al., 1995; Stammers et
102 al., 2001; Wong et al., 2007). Because these molecular genetic details of the transcriptional regulation
103 and associated factors are available, we used the bidirectional promoter region of the divergently
104 transcribed nitrate reductase (*niaD*) and nitrite reductae (*niiA*) genes as a model for the establishment
105 of CasID in this fungus. In this study we describe the establishment and the results of locus-specific
106 proteomics at the described *niiA-niaD* bidirectional promoter (from here on termed "intergenic
107 region", or "IGR") using the dCas9-guided proximity labelling approach and appropriate control strains.

108

109 **Material and Methods**

110 - Strains and growth conditions

111 #380 (additional wild type strain, no tag): *Aspergillus nidulans* wild type strain without any modification
112 used as a negative control for all other strains. Genotype: *yA2; biA1; veA1*

113 #871 (HA-AreA): *Aspergillus nidulans* strain with the transcription factor AreA tagged with 3xHA.
114 Genotype: *HA-AreA, pyroA1 or pyroA4, argB2, biA1, nku::bar, wA1*

115 #880 (CasID -sgRNA): in the strain #871, the TurboID-dCas fusion protein construct was introduced,
116 but not the sgRNA expressing construct. Genotype: *HA-AreA, pyroA1 or pyroA4, argB2::pTurboID-*
117 *dCas9, biA1, nku::bar, wA1*

118 #881 (CasID +sgRNA): Based on strain #880 that already expressed the TurboID-dCas fusion protein, a
119 constract expressing an sgRNA that targets the TurboID-dCas fusion protein to the *niiA-niaD* promoter
120 region next to AreA binding site 4 (see Fig 1). Genotype: *HA-areA, pyroA1 or pyroA4, argB2::pTurboID-*
121 *dCas9&revsgRNA-nirAII/areAIV, biA1, nku::bar, wA1*

122 - Preparation of the TurboID-dCas plasmids for transformation

123 As backbone of the TurboID-dCas plasmid, dmWt4-BirA_5 was digested with EcoRI (Schüller et al.,
124 2020). Primers which were used for construction of the plasmid are listed in Supplementary File 1.

125 <u>Construction of sgRNA-nirAII/AreAIV:</u>

126 The sgRNA was constructed analogous to Schüller et al. (2020) using the primers dCas9-gRNA-
127 areA4_nirAII-fwd-Afum and dCas9-gRNA-areA4_nirAII-rev-Afum.

128 The fragments were annealed using annealing buffer (10 mM Tris, pH 7.5 - 8.0, 50 mM NaCl, 1 mM
129 EDTA) in the PCR cycler. The Plasmids were generated by yeast recombinational cloning and introduced
130 in *A. nidulans* ectopically.

131 - Proximity biotinylation assay

132 All tested strains were plated on AMM+NO_3 and the respective supplements followed by incubation
133 at 37°C for 3 to 5 days. The spores were harvested with 5 ml 0.1% Tween 20 and filtered through glass

134 wool. To homogenize the spores in the suspensions, they were mixed for 6 hours at 4°C on a rotary
135 wheel. In a 1000 mL shake flask 200 mL AMM with appropriate auxotrophic supplements, 10mM
136 proline as neutral N-source for growth, 1nM DES for TurboID-dCas induction were inoculated with
137 $4*10^6$ spores/ mL and incubated at 37°C, 180 rpm for 17 hours. After this initial growth phase, 100 µM
138 biotin was added to provide sufficient biotin for the biotinylation reaction. To modulate AreA activity,
139 $NaNO_3^-$ was added to a final concentration of 150 µM for AreA activation or NH_4^+ tartrate to a final
140 concentration of 5 mM for AreA inactivation. Amended cultures were then further incubated for 1h at
141 37°C, 180 rpm. Finally, the samples were harvested using Miracloth filter (Merck), washed with sterile
142 tap water to remove extracellular biotin and then frozen in liquid nitrogen. The samples were
143 homogenized using Retsch mill (f = 30 s^{-1}, 30 sec).

144 - Protein extraction

145 For protein extraction 100 mg of the pulverized mycelium were put in a 2 ml tube. Protein extraction
146 buffer: 20 mM HEPES pH 7.5, 5 mM $MgCl_2$, 10 mM KCl, 2 mM EDTA, 1 mM DTT (prepare fresh!), 0.1
147 mM PMSF (in DMSO), 1 µM Leupeptin, 1 µM Pepstatin, 20% Glycerol. 1 ml buffer was added and the
148 cells were lysed using a Bioruptor (3 x 30 seconds, 30 seconds break in between the pulses) followed
149 by centrifugation at 15000 rpm for 10 min at 4°C. The supernatant was transferred to a new tube. To
150 remove previously intracellularly available biotin the buffer was exchanged using Amicon 10 kDa
151 columns according to the manufacturer´s instructions.

152 - Western blot

153 Equal amounts of the samples were loaded on a 10% SDS-PAGE and run at 160 V for 1 h. For the
154 transfer of the proteins to the membrane, Trans-Blot® Turbo™ transfer system (BioRad) was used at
155 25V, 2.5A, 20 min. The membrane was blocked with 3% BSA in TBST overnight followed by washing of
156 the membrane with TBST for 5 minutes. Subsequently the primary antibody (HA, Streptactin-HRP or
157 Cas9) in 3% BSA was added and the samples were incubated for 1h. The membrane was washed three
158 times with TBST for 15 minutes, respectively. The secondary antibody was added and incubated for

159 one hour. The membrane was washed again with TBST three times for 15 minutes, respectively, before
160 developing and visualization.

161 - Chromatin immunoprecipitation and qPCR

162 For chromatin immunoprecipitation the CasID test strains, AreA-HA as well as an untagged wild type
163 were used. All tested strains were inoculated in Aspergillus minimal media (AMM) with glucose as C-
164 source, 10 mM proline as N-source as well as the respective supplements. After incubation for 17 hours
165 at 37°C, 180 rpm, 100 µM biotin, 150 µM $NaNO_3$ for short-term induction or 10 mM NH_4^+ for short-
166 term repression as well as 1 nM diethylstilbestrol (DES) for TurboID-dCas induction were added to the
167 medium. These cultures were then incubated for one hour at 37°C, 180 rpm. For crosslinking,
168 formaldehyde (1% final concentration) was added followed by incubation at 20°C, 180 rpm for 15
169 minutes followed by addition of 125 mM glycine and incubation at 37°C, 180 rpm for 5 minutes. The
170 mycelia were harvested, washed with water to remove excess of biotin and frozen in liquid nitrogen
171 followed by pulverization using Retsch mill MM 400.

172 For the ChIP ~30 mg of the ground mycelia were put in a tube and 1 ml ChIP lysis buffer (50 mM Hepes-
173 KOH pH 7.5, 140 mM NaCl, 1 mM EDTA pH 8.0, 1% Triton X-100, 0.1% sodium deoxycholate and 0.1%
174 SDS + protease inhibitors) was added. The mycelia were sonicated for 25 minutes (2 minutes pulse, 1
175 minute break). The samples were centrifuged for one minute followed by transfer of the upper phase
176 to a fresh tube. Protein G agarose (ThermoFisher) was equilibrated with ten-fold volume of ChIP lysis
177 buffer. 40 µl of equilibrated protein G were added to the samples which were incubated at 4°C, 16
178 rpm, for 1 hour, followed by centrifugation and transfer of the liquid phase to a new tube. The sample
179 was split in 100 µl aliquots to which 900 µl dilution buffer (0.5% Triton X-100, 0.5% sodium
180 deoxycholate, 2 mM EDTA pH 8.0, 20 mM Tris-HCl pH 8.0, 150 mM NaCl) were added. 100 µl of one
181 dilution were taken aside as input control and kept at -80°C until reverse crosslinking. To the remaining
182 900 µl of the sample 1 µg antibody (Cas9 or HA) was added followed by incubation at 4°C, 16 rpm
183 overnight.

184 For precipitation of the protein-antibody conjugate, 40 µl Dynabeads™ Protein G for
185 immunoprecipitation (ThermoFisher) were added. The samples were incubated for 40 minutes at 4°C.
186 The tubes were put on a magnetic rack until the beads were settled and the liquid phase was removed.
187 Subsequently, the beads were washed three times with low salt buffer (0.5% Triton X-100, 0.5% sodium
188 deoxycholate, 2 mM EDTA pH 8.0, 20 mM Tris-HCl pH 8.0, 150 mM NaCl) and one time with high salt
189 buffer (0.5% Triton X-100, 0.5% sodium deoxycholate, 2 mM EDTA pH 8.0, 20 mM Tris-HCl pH 8.0, 500
190 mM NaCl). The beads were resuspended in 125 µl TES buffer (50 mM Tris-HCl pH 8.0, 10 mM EDTA pH
191 8.0, 1% SDS) and incubated overnight at 65°C, 850 rpm. 120 µl of the ChIP samples and 100 µl of the
192 input control, respectively, were transferred and 8.0 or 9.6 µl TEP buffer (167 mM EDTA pH 8.0, 667
193 mM Tris-HCl pH 8.0, 150 U/ml proteinase K) were added. After settling of the beads in a magnetic rack
194 the supernatant was transferred to a new tube followed by DNA purification (Quiagen, Mini Elute).

195 For the qPCR primers ChIP nirA2/areA4 1F (5´-CGCAATGGACGACCGTCATCG-3´) and ChIP nirA2/areA4
196 1R (5´-ATCAGAACGCTGCCCTGAGC-3´) were used.

197 - Enrichment of biotinylated proteins and tryptic digest

198 After extraction, the protein extracts were loaded on Sera-Mag™ SpeedBead Streptavidin-Blocked
199 Magnetic Particles which were previously blocked by washing with 3% BSA in TBST solution. After
200 incubating for one hour on the rotary wheel, unbound proteins were removed followed by different
201 washing steps as described by (Branon et al., 2018): 2x with cold extraction buffer, 1x with cold 1 M
202 KCl, 1x with cold 100 mM Na_2CO_3, 1x with 2M Urea in 10 mM Tris pH 8 and 2x with cold extraction
203 buffer without protease inhibitors and PMSF. After washing the beads five times, the beads were
204 suspended in 200 µl buffer containing 100 mM KCl.

205 The beads were washed three times with 45 µl 100 mM TEAB followed by alkylation and tryptic digest
206 according to the manufacturer´s instructions. Subsequently, the peptides were purified using C18 spin
207 tips. The samples were suspended in 8 µl 0.1% TFA followed by injection of 6 µl to the MS.

208

209 **Results**

210 - **Construction of the CasID strain and appropriate control strains**

211 To establish the method with the appropriate controls, a CasID test strain which contained TurboID-
212 dCas, the sgRNA and the HA-tagged AreA (CasID +sgRNA) was constructed. As control strains we
213 generated one strain where only AreA was HA-tagged as well as one additional control strain which
214 had the AreA-HA and also the TurboID-dCas construct but which lacked the sgRNA (CasID -sgRNA), that
215 would be necessary to bring TurboID-dCas at the desired locus of the IGR bidirectional nitrate
216 promoter. In addition, a wild type strain lacking all constructs also served as control. This latter strain
217 provides a negative control for all experiments including Westerns, ChIP experiments and proteomics
218 and also gives an indication for natively biotinylated or unspecific proteins that may bind to the affinity
219 column. The HA-AreA strain serves as control for the Western and ChIP analysis to confirm
220 transcription factor presence at the IGR target locus and again for natively biotinylated or unspecific
221 proteins binding to the affinity resin. The CasID -sgRNA control strain covers all aforementioned
222 unspecific proteins, but also reveals proteins that are biotinylated by the TurboID-dCas during all stages
223 from ribosomal generation until nuclear accumulation. In this case we should find an overlap with the
224 wild type and the HA-AreA strain and additionally find novel biotinylated proteins from various
225 compartments of the fungal cell. Finally, the CasID +sgRNA test strain directing the dCas fusion protein
226 to the selected IGR location in vicinity to the AreA-binding site 4 should add the final set of novel
227 proteins that are present and biotinylated specifically at that locus. TurboID-dCas as well as the sgRNA
228 constructs were ectopically integrated. All strains used for the experimental work are listed in Figure
229 2. They were tested for apparent phenotypes and showed comparable radial growth to the wild type
230 on minimal media containing either nitrate or ammonium (Supplementary Figure 1).

231 A scheme of the workflow and controls for CasID is shown in Figure 1.

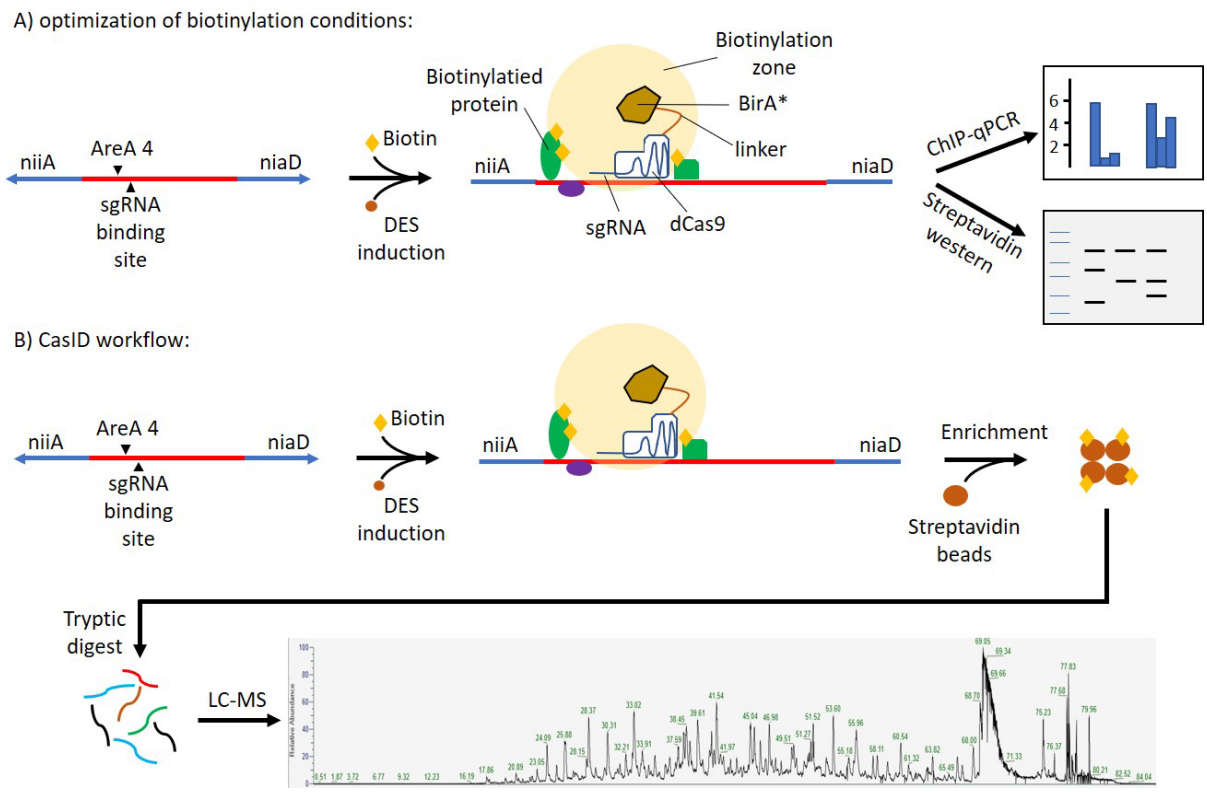

Figure 1: Workflow for optimization of biotinylation conditions (A) and the CasID workflow (B)

- **Localization of AreA and CasID under activating and repressing conditions**

In order to obtain proof of concept for the method, we wanted to create conditions where AreA as well as our TurboID-dCas fusion protein are both binding to the bidirectional nitrate promoter in close vicinity. This spacial neighborhood was desired as the TurboID part of the fusion protein has a limited functional radius of about 30nm that is mainly provided by the linker region between the TurboID and the dCas peptides (Fig. 1) (May et al., 2020). Therefore biotinylation of AreA by TurboID-dCas would only be feasible when both proteins are positioned next to each other. In our case, a suitable sgRNA PAM-motif is located at a 28 bp - or roughly 10nm - distance from AreA binding site 4 in the IGR (see Fig. 1) and this sequence was therefore chosen as a target locus. Besides the CasID +sgRNA test strain (strain 881) the CasID -sgRNA control strain (strain 880), and the control strain expressing only HA-AreA (strain 871) were used. As negative control for all strains, a wild type strain (strain 380) was grown in parallel. All of these strains were pre-grown on a neutral nitrogen source (proline) and then switched

248 to AreA-activating conditions by addition of 150 µM nitrate and further growth for 1 h. This low nitrate
249 pulse induction for 1 h was chosen to promote AreA binding and activity at the nitrate locus but avoid
250 high levels of the ammonium product that would lead to nitrogen metabolite repression and thus AreA
251 inactivation and export from the nucleus due to the activity of the CrmA exportin (Todd et al., 2005).

252 Following these consideration, we then performed a set of chromatin immunoprecipitation (ChIP)
253 experiments with all strains to test for the presence of HA-AreA and TurboID-dCas at the nitrate locus.
254 In these ChIPs, AreA was precipitated with an HA-specific antibody and the TurboID-dCas presence was
255 tested using a Cas9-specific antibody. Quantification of binding was carried out by qPCR using a set of
256 primer that encompass both binding sites. **Figure *2*** shows that AreA is strongly enriched at the nitrate
257 locus in the presence of nitrate in all strains that carry the construct (tester strain 881, control strains
258 880 and 871), but not in the wild type without HA-AreA (strain 380). Whereas AreA is highly enriched
259 in nitrate conditions, it is much less abundant when ammonium served as nitrogen source. This
260 confirms our previous data and also proves that the experimental set-up is correct for the subsequent
261 CasID development. ChIP results for TurboID-dCas binding at the nitrate promoter were only positive
262 in the CasID test strain (881) that contains the TurboID-dCas plus the sgRNA, but not in the control
263 strain (880) where no sgRNA is expressed. As expected, the TurboID-dCas protein was present in the
264 881 test strain at the nitrate locus under both nitrate-inducing and ammonium-repressing conditions
265 as the TurboID-dCas binding is not expected to be nitrogen source dependent. Interestingly, the
266 estrogen-dependent transcription of the TurboID-dCas gene seems to be leaky in the actual integration
267 locus as binding of the fusion protein was detected in comparable amounts regardless if DES was added
268 to the culture or not (compare lanes 881 $NaNO_3$ and 881 $NaNO_3$-DES in Fig. 3 (left)). In summary, these
269 ChIP experiments provided strong evidence that the system works as expected in the CasID test strain
270 and all control strains provide appropriate experimental controls to move forward with the method
271 development.

272

Strain	Supplements	DES	$NaNO_3$ / NH_4^+	AreA	CAS
380 (wt)	arg, bio	+	$NaNO_3$	no	no
871 (AreA-HA)	arg, bio, pyro	+	$NaNO_3$	yes	no
871 (AreA-HA)	arg, bio, pyro	+	NH_4^+	no	no
880 (CasID-sgRNA)	bio, pyro	+	$NaNO_3$	yes	no
880 (CasID-sgRNA)	bio, pyro	+	NH_4^+	no	no
881 (CasID+sgRNA)	bio, pyro	+	$NaNO_3$	yes	yes
881 (CasID+sgRNA)	bio, pyro	+	NH_4^+	no	yes
881 (CasID+sgRNA)	bio, pyro	-	$NaNO_3$	yes	no/yes

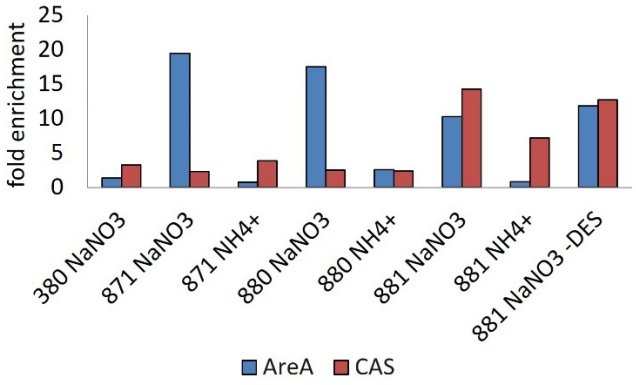

Figure 2: Enrichment of AreA and TurboID-dCas at the nitrate locus under different conditions; 380 wild type (wt) control strain; 871: control strain with HA-tagged AreA; 880: control stain with HA-tagged AreA and CasID-sgRNA; 881: CasID test strain with HA-tagged AreA and CasID+sgRNA; TurboID-dCas and sgRNA directing it to the nitrate promoter 30 bp apart from AreA binding site 4.

- **Optimization of biotinylation conditions and Western analysis of products**

With the confirmation that both proteins are at the locus of interest close to each other one hour after induction, biotinylation of AreA may occur. Since all strains except the wild type control contain an HA-tagged AreA, we were able detect this protein by western blots and at the same time probe for biotinylation using a streptactin-HRP detection system. We reasoned that AreA may be biotinylated in the CasID samples and hence there might be an overlap between the HA-derived signal for AreA and a band from the biotinylation assay. In the western blot in **Figure *3***, left panel (streptactin-HRP) biotinylated proteins are revealed. There are several bands visible in all strains (e.g. strong band at around 130 kDa) indicating that these proteins are natively biotinylated in *A.nidulans*. But there are also a few bands visible exclusively in the samples derived from TurboID-dCas containing strains (880, 881). This indicates that the TurboID-dCas fusion protein is functional and biotinylates closely spaced

289 proteins via the Turbo-BirA enzyme. Most of these additional bands appear in the biotinylation assay
290 regardless whether the fusion protein is targeted to the locus (CasID strain 881) or not (control strain
291 880). However, there are two bands at an apparent size between 30 kDa and 55 kDa visible in this
292 Western blot that specifically appear only in the CasID strain with the sgRNA indicating a successful
293 biotinylation reaction at the nitrate locus. None of these bands, however, would correspond to the
294 expected full size of an AreA monomer of 94 kDa.

295 The HA-specific Western for the detection of the corresponding AreA band, however, did not show a
296 signal at the expected size of 94 kDa but four signals with lower molecular weight starting at 55 kDa
297 and lower appeared in the HA-AreA carrying strains. These signals were not present in the wild type
298 control (lane HA- in Fig 3, central panel) and thus appear to be specific processing or degradation
299 products of HA-AreA. Interestingly, two of the four bands (55 kDa and slightly below at around 50kDa)
300 are also strongly stained on the streptactin western blot in the CasID strain (labelled +sgRNA) and
301 weakly in the control strain with TurboID-dCas without sgRNA (labelled -sgRNA). Although these
302 similarities between the two western blots could indicate biotinylation of HA-AreA (before processing
303 or degradation), similar sizes of the signals could also be pure coincidence and thus it is advisable to
304 avoid any conclusions before an independent method, e.g. mass spectrometry analysis of biotinylated
305 proteins, would have confirmed these data.

306

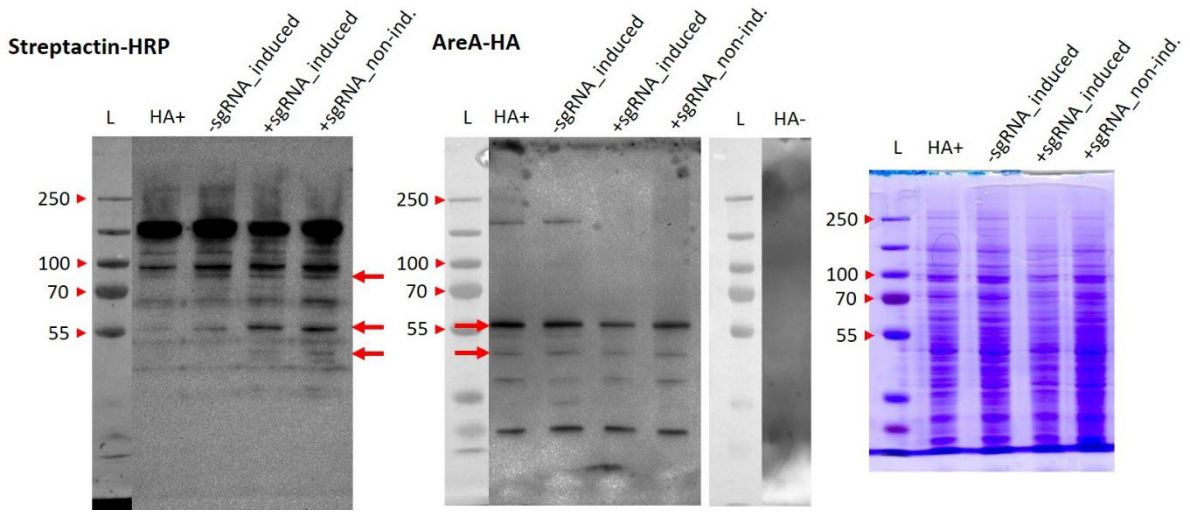

Figure 3: Western blots for the detection of biotinylated proteins via streptactin-HRP (left), the HA.tagged AreA (middle) and a coomassie stained SDS-PAGE as loading control (right). HA+: strain 871 containing only the HA-AreA construct; -sgRNA_induced: strain 880 containing TurboID-dCas without sgRNA grown in the presence of 10nM DES inducer for the TurboID-dCas construct; +sgRNA_induced: strain 881 containing TurboID-dCas and also the sgRNA targeting the construct to the nitrate locus, grown in the presence of 10nM DES; +sgRNA_non-ind.: strain 881 containing TurboID-dCas and also the sgRNA, grown without inducer for the TurboID-dCas construct (note that expression of the construct is leaky and also occurs to some extent in the absence of inducer)

- **Enrichment and protein mass spectrometry analysis of biotinylation of products**

To obtain a comprehensive view on specific proteins present at the chromatin of the selected locus, the method of choice is protein mass spectrometry of protein extracts that were enriched for biotinylated proteins by affinity purification. The detailed steps of the procedure are described in the Materials and Methods section, but briefly, proteins were extracted from mycelia of the CasID strain and from the control strains using a standard native protein extraction protocol. After this step, protein extracts were loaded on streptavidin coated magnetic beads and washed extensively using different buffers to elute non-specifically attaching proteins from the streptavidin-coated matrix. Optimally, after these washing steps, only biotinylated proteins should remain bound to the beads. Because of the exceptionally high affinity between biotin and streptavidin ($K_d \sim 10^{-14}$ M) elution of the bound proteins is only feasible under chemically denaturing conditions and high temperatures (Deng et al., 2013). Moreover, it is known that biotinylation of lysine drastically reduces the efficiency of trypsin to cleave after the biotinylated lysine residue (Li et al., 2021). To circumvent these problems, a two-step elution of streptavidin-bound proteins was pursued. In the first step, beads were subjected to tryptic

330 digest directly in the suspension to release peptides that can be cut at arginines or non-biotinylated
331 lysines. In the second step, the remaining peptides bound via their biotinylated lysine(s) to the
332 streptavidin-coated beads were eluted using excess of biotin and denaturing, but still MS-compatible
333 conditions. Both elution samples were subsequently combined and subjected to MS analysis.

334 The LC-MS analysis was done from two biologically and technically independent extractions and
335 enrichments. To our surprise, the number of total proteins detected in all control strains, was quite
336 high and was in the range between 800 – 900 different proteins detected already in the control
337 samples. Only in the CasID strain, the number of total proteins detected by MS was slightly higher and
338 in the range between 1.100 – 1.400 different proteins (Table 1). These MS results indicated that despite
339 several rigorous washing steps, the number of proteins unspecifically attaching to the streptavidin-
340 coated beads is very high. Several attempts using different buffers and washing conditions based on
341 published protocols and a literature search revealed that this problem existed also in many other
342 studies using this enrichment method (reviewed in (Trinkle-Mulcahy, 2019). Therefore, a set of
343 rigorous genetic and experimental controls is necessary that allows to discriminate the specific
344 proteins labelled by the TurboID-dCas enzyme from the general background during enrichment.

345

346

347

348

349 *Table 1: Summary of identified proteins with and without biotinylation; AreA-HA is the HA-tagged control strain, CasID-*
350 *sgRNA contains the biotin ligase fused to cas9 without sgRNA (background biotinylation), CasID+sgRNA also contains a*
351 *sgRNA*

Sample name	Number of identified proteins w/o biotinylation	Number of identified proteins with biotinylation	Total Number of identified proteins
AreA-HA_1	916	3	919
CasID-sgRNA_1	983	5	988
CasID+sgRNA_1	1119	5	1124
AreA-HA_2	909	7	916
CasID-sgRNA_2	852	2	854
CasID+sgRNA_2	1433	4	1437

352

353 In the two independent measurements of each strain a partially different protein profile was detected,
354 however, the majority of the proteins within the replicates was identical in both biologically
355 independent experiments.

356 Surprisingly, proteins carrying a biotinylation were hardly detected in any sample. **Figure 4A** shows a
357 Venn diagram derived from Table 1 where the proteins carrying a biotin moiety from the different
358 strains are visualized. We found six "natively biotinylated" proteins that appeared in all analyzed
359 strains at least in one of the two replicates **(Figure 4B)**. For some of these proteins, like biotin
360 carboxylase or pyruvate carboxylase, biotinylation is a known posttranslational modification. Others,
361 like AN4308 (predicted translation protein), AN3636 (predicted phosphatidyl-inositol phospholipase C,
362 an enzyme known to be involved in signal transduction) or AN1394 (predicted septin type G-protein
363 cytoskeletal protein) are so far not known to carry biotin as a PTM and the significance of this finding
364 needs to be validated by additional repetitions testing also other genetic backgrounds.

365 Another six proteins appeared to be biotinylated exclusively in the CasID test strain expressing
366 TurboID+sgRNA. In this population of biotinylated peptides we expected mainly proteins that are
367 known to associate with chromatin. The identity of these proteins, however, is quite divers.

A)

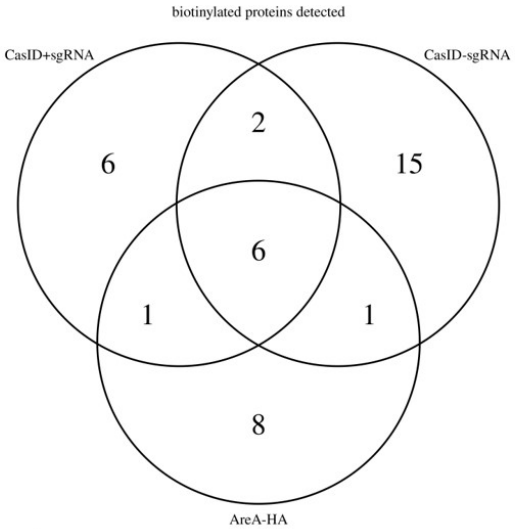

B)

all strains	proteinID	gene ID	function
	A0A1U8QL21	AN6126	Biotin carboxylase OS=Emericella nidulans (strain FGSC A4 / ATCC 38163 / CBS 112.46 / NRRL 194 / M139) OX=227321 GN=AN6126.2 PE=4 SV=1
	A0A1U8QYE9	AN4308	Translation protein OS=Emericella nidulans (strain FGSC A4 / ATCC 38163 / CBS 112.46 / NRRL 194 / M139) OX=227321 GN=AN4308.2 PE=3 SV=1
	A0A1U8QUD8	AN3636	PLCXc domain-containing protein OS=Emericella nidulans (strain FGSC A4 / ATCC 38163 / CBS 112.46 / NRRL 194 / M139) OX=227321 GN=AN3636.2 PE=4 SV=1
	G5EB39	AN1394	Septin-type G domain-containing protein OS=Emericella nidulans (strain FGSC A4 / ATCC 38163 / CBS 112.46 / NRRL 194 / M139) OX=227321 GN=ANIA_01394 PE=3 SV=1
	Q5B440	AN4690	3-methylcrotonyl-CoA carboxylase biotin-containig subunit3-methylcrotonyl-CoA carboxylase biotin-containing subunit OS=Emericella nidulans (strain FGSC A4 / ATCC 38163 / CBS 112.46 / NRRL 194 / M139) OX=227321 GN=ANIA_04690 PE=4 SV=1
	Q5B4R8	AN4462	Pyruvate carboxylase OS=Emericella nidulans (strain FGSC A4 / ATCC 38163 / CBS 112.46 / NRRL 194 / M139) OX=227321 GN=ANIA_04462 PE=4 SV=1
only CasID+sgRNA	**proteinID**	**gene ID**	**function**
	Q5B5G2	AN4218	Elongation factor 1-alpha OS=Emericella nidulans (strain FGSC A4 / ATCC 38163 / CBS 112.46 / NRRL 194 / M139) OX=227321 GN=AN4218.2 PE=3 SV=1
	Q5B706	AN3674	Hypothetical PH domain protein (Eurofung) OS=Emericella nidulans (strain FGSC A4 / ATCC 38163 / CBS 112.46 / NRRL 194 / M139) OX=227321 GN=ANIA_03674 PE=4 SV=1
	Q5B8E2	AN3188	Phosphatidylserine decarboxylase proenzyme 2 OS=Emericella nidulans (strain FGSC A4 / ATCC 38163 / CBS 112.46 / NRRL 194 / M139) OX=227321 GN=PSD2 PE=3 SV=1
	A0A1U8QX88	AN1935	Calponin-homology (CH) domain-containing protein OS=Emericella nidulans (strain FGSC A4 / ATCC 38163 / CBS 112.46 / NRRL 194 / M139) OX=227321 GN=AN1935.2 PE=4 SV=1
	A0A1U8QK56	AN5912	ADP-ribosylation factor-like protein 1 OS=Emericella nidulans (strain FGSC A4 / ATCC 38163 / CBS 112.46 / NRRL 194 / M139) OX=227321 GN=AN5912.2 PE=3 SV=1
	C8V131	AN6595	Acyl-CoA dehydrogenase NM domain-like protein OS=Emericella nidulans (strain FGSC A4 / ATCC 38163 / CBS 112.46 / NRRL 194 / M139) OX=227321 GN=ANIA_10834 PE=3 SV=1

368

369

370 *Figure 4: Venn diagrams of biotinylated proteins identified in at least one of the two independent measurements of the strains*

371 For example, we find biotinylated elongation factor 1 alpha (gene AN4218) that could have been
372 biotinylated during the process of translating TurboID-dCas9. A calponin-homology domain containing
373 protein (gene AN1935), known for its actin binding capacities (Yin et al., 2020), could have been at the
374 chromatin locus, as well as AN3674, a pleckstrin-homology domain (PH) protein that is also related to

375 cytoskeletal function and membrane targeting and AN5912, that encodes a predicted GTPase
376 regulating vesicle formation during intracellular traffic and also related to processes in which PH
377 proteins are involved. (Lemmon, 2004) On the other hand, there is no obvious “chromatin-connection”
378 to the AN3188 product that is predicted to be involved in phospholipid metabolism, and AN6595 that
379 codes for a predicted acylCoA-DH enzyme involved in peroxisomal beta oxidation of fatty acids.
380 Overall, these six proteins for which biotinylated peptides have been identified by MS at least in one
381 of the experiments have some known chromatin-related functions but each of these proteins should
382 be independently validated by tagging, purification and MS analysis identifying the biotinylation status.
383 rather represent proteins that were biotinylated during the transit of the TurboID-dCas9 protein from
384 the site of translation to the nucleus and further to the target site at the nitrate promoter.

385 In order to improve the selectivity of our analyses for specific proteins only appearing in the
386 CasID+sgRNA strain we restricted all MS peptide hits to those that appeared in both independent
387 measurements of each strain, but regardless if these proteins are biotinylated or not as the biotin
388 moiety may still be bound to the streptavidin beats after the tryptic digest and also not been eluted in
389 the second step (Figure 5).

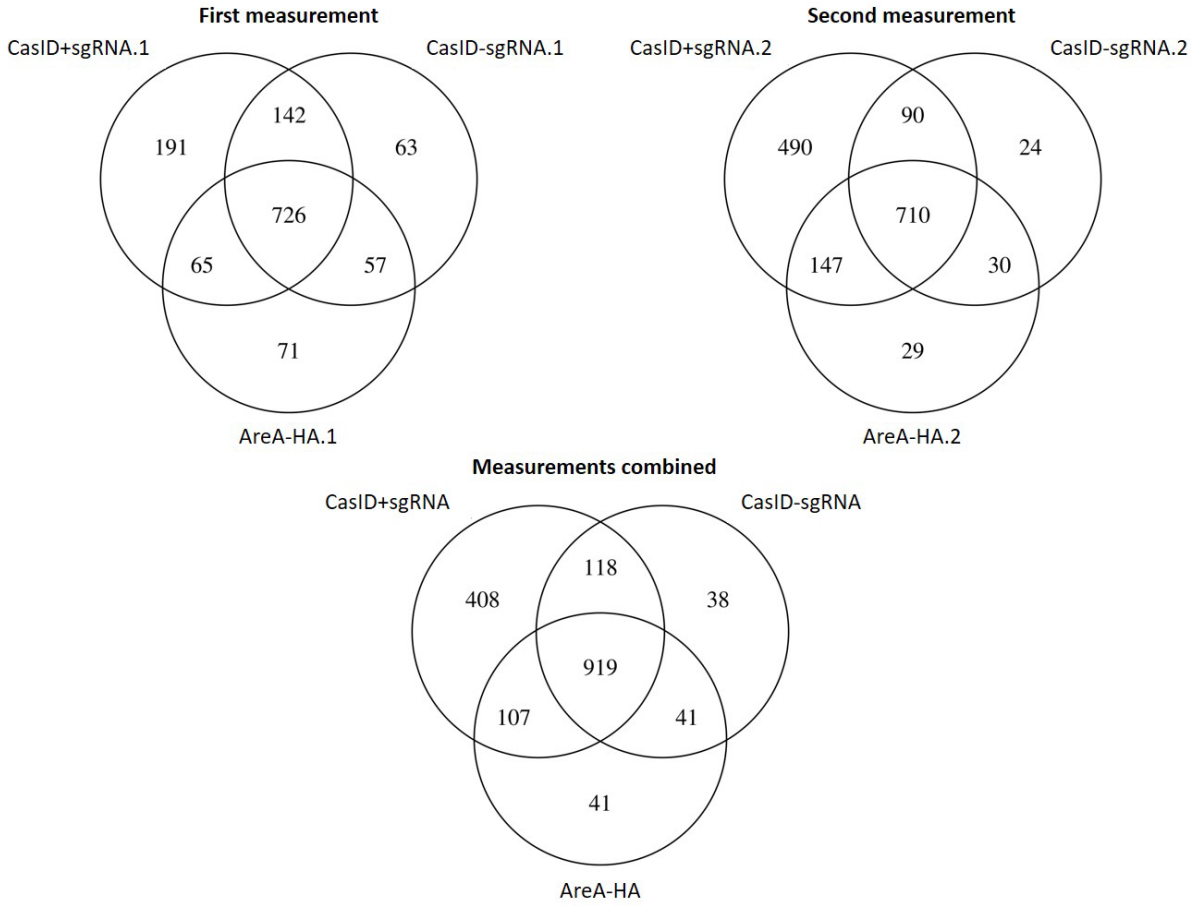

Figure 5: Venn diagrams of proteins identified in the two independent measurements of the strains and of both measurements combined

While in the first measurement only 191 proteins were exclusively present in the CasID+sgRNA strain, in the second approach 490 proteins were identified. After merging the protein IDs of both measurements 408 proteins appeared at least once and only 32 of them were detected in both measurements specifically in the CasID+sgRNA strain. A complete list of these 32 consistently detected proteins with their proposed function is shown in Table 2. There are several putative and uncharacterized proteins included but also a few with an already described function. The accessions highlighted in red font are known to be located in the nucleus. Among the already characterized proteins are PhnA (gene ANIA_00082), a phosducin like protein required for vegetative growth, developmental control, and toxin biosynthesis, BudA (gene ANIA_01324) involved in septum

403 formation, CmkB (gene ANIA_03065) a calmodulin dependent protein kinase. Strikingly, we also found
404 NmrA (gene ANIA_08168), a regulatory protein negatively regulating AreA activity. NmrA interacts with
405 AreA at its C- as well N-terminus and thereby blocks its activity und nitrogen metabolite repressive
406 conditions. AreA itself was not among the proteins falling into the selection category (only in the
407 CasID+sgRNA in both independent repetitions), although it was detected in one of the experiments in
408 this strain.

409 *Table 2: Genes where corresponding proteins were exclusively identified in the CasID strain; bold = characterized proteins;*
410 *red = known nuclear proteins*

Gene	**Function**
ANIA_00082	PhnA: phosducin like protein; required for Gβγ-mediated signaling for vegetative growth, developmental control, and toxin biosynthesis
ANIA_00789	Hypothetical protein; Orthology: E2 ubiquitin-conjugating enzyme
ANIA_01324	BudA*:* functions at sites of septum formation
ANIA_01525	Hypothetical protein; Orthologs: Signal peptidase complex subunit 2
ANIA_01768	Hypothetical protein; VHS domain-containing protein
ANIA_01973	v-SNARE protein VTI1; Ortholog(s) have SNAP receptor activity and role in Golgi to vacuole transport, intra-Golgi vesicle-mediated transport, vacuole fusion, non-autophagic, vesicle fusion
ANIA_02119	sphingolipid transporter; Ortholog(s) have sphingolipid transporter activity, role in sphingolipid metabolic process and fungal-type vacuole membrane localization
ANIA_02272	adenosine kinase; Putative kinase with a predicted role in ribose metabolism or nucleotide salvage pathways
ANIA_03065	calmodulin-dependent protein kinase CmkB
ANIA_10418	Hypothetical protein
ANIA_03910	Hypothetical protein; Sister chromatid separation protein, putative

ANIA_03944	Putative DNA-directed DNA polymerase phi Ortholog(s) have rDNA binding activity, role in transcription of nuclear large rRNA transcript from RNA polymerase I promoter and cytosol, nucleolus localization
ANIA_04189	putative mitogen-activated protein kinase kinase mkkA
ANIA_04265	condensin subunit BRN1; Ortholog(s) have ATPase activity, role in DNA repair, mitotic chromosome condensation and cytosol, nuclear condensin complex localization
ANIA_04278	1-phosphatidylinositol 4-kinase STT4; Essential 1-phosphatidylinositol 4-kinase with a predicted role in phospholipid metabolism
ANIA_04753	Hypothetical protein; Ortholog(s) have unfolded protein binding activity, role in mitochondrial respiratory chain complex IV assembly and integral component of membrane, mitochondrial inner membrane, plasma membrane localization
ANIA_04757	Ubiquinone biosynthesis protein coq4, mitochondrial
ANIA_05522	Hypothetical protein; Has domain(s) with predicted structural constituent of ribosome activity, role in translation and ribosome localization
ANIA_05536	GTPase NPA3; Ortholog(s) have cytosol localization; Orthologs: GPNloop GTPase
ANIA_05592	Rho family guanine nucleotide exchange factor CDC24
ANIA_05702	Hypothetical protein; Ortholog(s) have role in ribosomal large subunit biogenesis, ribosomal small subunit biogenesis and cytosolic large ribosomal subunit, nucleolus localization
ANIA_01745	Hypothetical protein; Serine hydroxymethyltransferase
ANIA_05900	Hypothetical protein; Orthologs: CUE domain containing protein, AMFR protein
ANIA_10762	DNA-directed DNA polymerase alpha catalytic subunit POL1; DNA-directed DNA polymerase
ANIA_06158	Hypothetical protein; Glutathione S-transferase, putative
ANIA_06741	Hypothetical protein; Ortholog(s) have polyubiquitin binding activity

ANIA_06986	*vnxA*; Ortholog(s) have calcium:proton antiporter activity, potassium:proton antiporter activity, sodium:proton antiporter activity and role in hydrogen transport, potassium ion transport, sodium ion transport
ANIA_07632	bifunctional alcohol dehydrogenase/S-(hydroxymethyl)glutathione dehydrogenase; Putative dehydrogenase with a predicted role in two-carbon compound metabolism
ANIA_07762	Hypothetical protein; Ortholog: RNA 3'-phosphate cyclase
ANIA_08168	NmrA; Regulatory protein involved in nitrogen metabolite repression
ANIA_10918	Hypothetical protein; Has domain(s) with predicted calcium ion binding, phosphatidylinositol binding activity and role in cell communication
ANIA_11347	Hypothetical protein; Ortholog(s) have cytochrome-c oxidase activity, role in mitochondrial electron transport, cytochrome c to oxygen and mitochondrial respiratory chain complex IV, plasma membrane localization

411

412 **Discussion and Conclusions**

413 For method development we targeted the fusion enzyme to the well characterized nitrate locus. This
414 locus was chosen due to the possibility of rigorous controls and the possibility to test CasID and an
415 adjacent regulator binding first by ChIP to see if the system works. MS results of the locus CasID
416 confirmed the ChIP data in two ways: (i) we found several chromatin-related proteins specifically only
417 in the CasID+sgRNA strain indicating that biotinylation occurred at the locus, and (ii) although we did
418 not consistently find our main target AreA as biotinylated protein in MS analysis, we found the AreA-
419 interacting regulator NmrA exclusivey in the CasID+sgRNA strain. At this point we can only speculate
420 on the significance of this finding, but it could be that the TurboID part of the fusion protein could
421 reach out and target the interacting NmrA, but not the "underlying" AreA regulator itself. In any case,
422 the result fits well with the known function of AreA regulation by NmrA. In addition, our data would
423 indicate that NmrA modulates AreA activity while always interacting with it, as we found this
424 interaction during nitrate conditions. This would mean that NmrA was already present at the locus

425 although not negatively interfering with AreA function. Future studies may be warranted that look into
426 this interaction in more detail. It could be that the biotinylation radius with the biotinyl-5´-AMP cloud
427 around the TurboID of CasID was too narrow to find also AreA. One possibility to enlarge the
428 biotinylation radius would be the introduction of a longer linker between dCas9 and TurboID allowing
429 more flexibility. Since DNA and chromatin are flexible structures, not static, it is also possible that AreA
430 was simply out of reach or that NmrA was closer to CasID and preventing AreA from being biotinylated.
431 In addition to a longer linker between sCas9 and TurboID, also the employment of more than one
432 sgRNAs per locus would be an alternative ("primer walking"). In our case, in the bidirectional promoter
433 between *niiA* and *niaD* there are ten binding sites for AreA and four binding sites for NirA described
434 (Muro-Pastor et al., 1999). By using this"primer walking" strategy setting sgRNAS around all AreA
435 binding sites more chromatin regulators of this locus could be identified.

436 Other characterized proteins consistently detected only in the CasID+sgRNA test strain at the selected
437 nitrate locus were were PhnA, BudA, or CmkB. PhnA is a phosducin-like protein which are described as
438 regulators of G-protein signaling disrupting the G-protein interaction of subunit Gα and Gβγ (Blüml et
439 al., 1997), and the predicted localization of PhnA using "WoLF PSORT Prediction"
440 (https://www.genscript.com/wolf-psort.html) is with the highest probability in the nucleus. Deletion
441 of the gene in *A. nidulans* results in reduced biomass, asexual sporulation in liquid submerged culture,
442 and defective fruiting body formation. Also mycotoxin production is strongly affected since *aflR* is no
443 longer transcribed in the deletion strain (Seo and Yu, 2006). Since we also detected PhnA here by CasID
444 at the nitrate locus it may play a general role in chromatin function. BudA belongs to the actin-binding
445 proteins and has been found in *A.nidulans* to function at sites of septum formation (Harris et al., 2009;
446 Virag and Harris, 2006). So presumably, this protein is not expected to reside at the nitrate locus,
447 however, fungi feature a special type of "open mitosis" in which the cytoskeleton, including actin,
448 reaches through the partially disassembled nuclear envelope to establish intimate contacts with the
449 segregating chromosomes (Boettcher and Barral, 2013). Mutants of Bud6, the BudA homolog of
450 *S.cerevisiae*, show defects in mitosis, possess fewer secretory vesicles, form abnormal septa, and

451 display abnormal actin bars in nuclei. As we also found cytoskeleton-associated proteins in the list of
452 biotinylated proteins specific for the CasID+sgRNA strain, we still need to consider BudA as true
453 chromatin-interacting protein captured at our target locus most likely during mitosis. Also the third
454 characterized protein identified in this CasID screen, CmkB has a role in mitosis and nuclear division. It
455 is a calmodulin-dependent kinase needed for the proper temporal activation of the main cell cycle
456 kinase NimX (CDC2) and timely progression of the nuclear division (Joseph and Means, 2000).

457 Overall, it seems that the our CasID strategy was successful in capturing an expected regulator at the
458 nitarte locus (NmrA) and several other chromatin-associated proteins such as a condensin subunit
459 (ANIA 04265), DNA polymerase (ANIA 03944), sister chromatid separation (ANIA 03910) and other
460 proteins that regulate mitosis and cell division. This high proportion of cell-cycle-associated proteins
461 might be due to the fact that our biotin-labelling time was over a period of roughly 12 hours and thus
462 several mitoses have certainly occurred during this time. This could lead to the observed biotinylation
463 of cytoskeletal proteins, as moreover, they are highly abundant in the nucleus during the cell division
464 process. As these proteins are most likely not really specific for the target locus, it will be necessary in
465 the future CasID approaches to shorten the labelling time of CasID at the locus. As we have a
466 conditional expression system for the TurboID-dCas9 construct and can also add the additional biotin
467 for a shorter time period, such time restriction of the biotinylation process is feasible. This adaptation
468 may lead to a more locus-specific labelling of the chromatin-associated proteome. Another abundant
469 family of detected prtoeins are related to membrane biogenetics and trafficking. This is also not
470 suprising, as it is known that mitotic exit (Davies et al., 2004) or active transcription locates large
471 genomic regions in close vicinity to the nuclear membrane and thus establishing an intimate
472 connection between membrane biology and the 3-dimensional genome architecture (Sosa Ponce et
473 al., 2024).

474 Certainly, a strong bottleneck of the CasID method is the enrichment of biotinylated proteins via the
475 strepatavidin-cated paramagnetic beads. This procedure leads to a high level of unspecific proteins
476 that adhere to the matrix without biotinylation and it has already been reported many times in the

477 literature, that some of these “contaminants” can not be eliminatedeven by extensive washing with
478 compatible buffer systems. Ideally, we would get a few biotinylated proteins, however, in every
479 measurement and sample beyond 800 proteins could be unambiguously identified. The high
480 background after enrichment has previously been documented as a challenge in several studies
481 (Branon et al., 2018; Mair et al., 2019; Zhang et al., 2020). As shown in Supplementary Figure 2 the
482 majority of the proteins were detected in both of the two independent measurements in the
483 respective strains. For example, 727 proteins were detected in both measurements in the AreA-HA
484 control strain which does not have the TurboID-dCas9 biotin ligase. In comparison, there were 1009
485 proteins identified in both measurements of our CasID+sgRNA test strain. After subtracting proteins
486 which were identified in all three control strains, only 32 proteins remained exclusively and
487 consistently detected in the CasID test strain.These results point out once more how crucial
488 appropriate controls are in proximity labelling experiments.

489 The goal of this study was to adapt the CasID method to identify chromatin-related proteomes at a
490 specific locus of interest in our model organism *A. nidulans*. One type of the loci to be studied in future
491 will be biosynthetic gene clusters (BGCs) encoding secondary metabolites. These genomic regions
492 seem to have a very specific chromatin landscape that is far from being understood at the molecular
493 level (Gacek and Strauss, 2012; Pfannenstiel and Keller, 2019) and thus CasID could help in identifying
494 new regulators. In all fungi studied so far, the majority of genomic clusters coding for secondary
495 metabolites (biosynthetic gene clusters, BGCs) are usually silenced by default during active growth
496 through heterochromatin structures (Atanasoff-Kardjalieff and Studt, 2022; Connolly et al., 2013;
497 Reyes-Dominguez et al., 2012; Soyer et al., 2014; Studt et al., 2016) and are only activated in response
498 to environmental or developmental signals but then often lack typical “active” chromatin signatures
499 like histone H3-lysine 4 methylation (Gacek-Matthews et al., 2016; Karahoda et al., 2022). Thus far,
500 BGC-specific components at a certain locus can only be studied by ChIP provided specific antibodies
501 are available for known posttranslational modifications or tagged proteins. CasID may help to identify
502 new regulatory components at loci of interest as it can be employed to identify parts of the condition-

503 specific proteome in a high spatial resolution using different sgRNAs for targeting the dCas-BirA fusion
504 enzyme. Nevertheless, we need to be aware that this method can give us a first information on proteins
505 potentially present at a locus and additional verification and confirmation is indispensable.

506

507

508 **Acknowledgments**

509 This work was supported by grant Nr. P32790-B of the Austrian Science Fund FWF to JS .

510 **Author contributions:** TS – experimental design and execution, data evaluation, preparation of the
511 draft manuscript; DNL – experimental design and execution, data evaluation; AS – Preparation of the
512 test strains; KH, SS and ERF – proteomics analysis; JS – Experimental design, data analysis and
513 evaluation, funding acquisition

514 **References**

515 Anton, T., Karg, E., Bultmann, S., 2018. Applications of the CRISPR/Cas system beyond gene editing.
516 Biol. Methods Protoc. 3, bpy002. https://doi.org/10.1093/biomethods/bpy002
517 Blüml, K., Schnepp, W., Schröder, S., Beyermann, M., Macias, M., Oschkinat, H., Lohse, M.J., 1997. A
518 small region in phosducin inhibits G-protein betagamma-subunit function. EMBO J. 16, 4908–
519 4915. https://doi.org/10.1093/emboj/16.16.4908
520 Branon, T.C., Bosch, J.A., Sanchez, A.D., Udeshi, N.D., Svinkina, T., Carr, S.A., Feldman, J.L., Perrimon,
521 N., Ting, A.Y., 2018. Efficient proximity labeling in living cells and organisms with TurboID.
522 Nat. Biotechnol. 36, 880–887. https://doi.org/10.1038/nbt.4201
523 Caesar, L.K., Kelleher, N.L., Keller, N.P., 2020. In the fungus where it happens: history and future
524 propelling Aspergillus nidulans as the archetype of natural products research. Fungal Genet.
525 Biol. FG B 144, 103477. https://doi.org/10.1016/j.fgb.2020.103477
526 Cho, K.F., Branon, T.C., Udeshi, N.D., Myers, S.A., Carr, S.A., Ting, A.Y., 2020. Proximity labeling in
527 mammalian cells with TurboID and split-TurboID. Nat. Protoc. 15, 3971–3999.
528 https://doi.org/10.1038/s41596-020-0399-0
529 Drott, M.T., Bastos, R.W., Rokas, A., Ries, L.N.A., Gabaldón, T., Goldman, G.H., Keller, N.P., Greco, C.,
530 2020. Diversity of Secondary Metabolism in Aspergillus nidulans Clinical Isolates. mSphere 5,
531 e00156-20. https://doi.org/10.1128/mSphere.00156-20
532 Gawlik, J., Koper, M., Bogdanowicz, A., Weglenski, P., Dzikowska, A., 2022. Nuclear Functions of
533 KaeA, a Subunit of the KEOPS Complex in Aspergillus nidulans. Int. J. Mol. Sci. 23, 11138.
534 https://doi.org/10.3390/ijms231911138
535 Han, X., Qiu, M., Wang, B., Yin, W.-B., Nie, X., Qin, Q., Ren, S., Yang, K., Zhang, F., Zhuang, Z., Wang,
536 S., 2016. Functional Analysis of the Nitrogen Metabolite Repression Regulator Gene nmrA in
537 Aspergillus flavus. Front. Microbiol. 7, 1794. https://doi.org/10.3389/fmicb.2016.01794
538 Inglis, D.O., Binkley, J., Skrzypek, M.S., Arnaud, M.B., Cerqueira, G.C., Shah, P., Wymore, F., Wortman,
539 J.R., Sherlock, G., 2013. Comprehensive annotation of secondary metabolite biosynthetic
540 genes and gene clusters of Aspergillus nidulans, A. fumigatus, A. niger and A. oryzae. BMC
541 Microbiol. 13, 91. https://doi.org/10.1186/1471-2180-13-91
542 Kong, Q., Chang, P.-K., Li, C., Hu, Z., Zheng, M., Sun, Q., Shan, S., 2020. Identification of AflR Binding
543 Sites in the Genome of Aspergillus flavus by ChIP-Seq. J. Fungi Basel Switz. 6, 52.
544 https://doi.org/10.3390/jof6020052
545 Lamb, H.K., Leslie, K., Dodds, A.L., Nutley, M., Cooper, A., Johnson, C., Thompson, P., Stammers, D.K.,
546 Hawkins, A.R., 2003. The negative transcriptional regulator NmrA discriminates between
547 oxidized and reduced dinucleotides. J. Biol. Chem. 278, 32107–32114.
548 https://doi.org/10.1074/jbc.M304104200
549 Lamb, H.K., Ren, J., Park, A., Johnson, C., Leslie, K., Cocklin, S., Thompson, P., Mee, C., Cooper, A.,
550 Stammers, D.K., Hawkins, A.R., 2004. Modulation of the ligand binding properties of the
551 transcription repressor NmrA by GATA-containing DNA and site-directed mutagenesis.
552 Protein Sci. Publ. Protein Soc. 13, 3127–3138. https://doi.org/10.1110/ps.04958904
553 Mair, A., Xu, S.-L., Branon, T.C., Ting, A.Y., Bergmann, D.C., n.d. Proximity labeling of protein
554 complexes and cell-type-specific organellar proteomes in Arabidopsis enabled by TurboID.
555 eLife 8, e47864. https://doi.org/10.7554/eLife.47864
556 Muro-Pastor, Mi., Gonzalez, R., Strauss, J., Narendja, F., Scazzocchio, C., 1999. The GATA factor AreA
557 is essential for chromatin remodelling in a eukaryotic bidirectional promoter. EMBO J. 18,
558 1584–1597. https://doi.org/10.1093/emboj/18.6.1584
559 Pan, H., Feng, B., Marzluf, G.A., 1997. Two distinct protein-protein interactions between the NIT2 and
560 NMR regulatory proteins are required to establish nitrogen metabolite repression in
561 Neurospora crassa. Mol. Microbiol. 26, 721–729. https://doi.org/10.1046/j.1365-
562 2958.1997.6041979.x
563 Pateman, J.A., Cove, D.J., 1967. Regulation of nitrate reduction in Aspergillus nidulans. Nature 215,
564 1234–1237. https://doi.org/10.1038/2151234a0

Punt, P.J., Strauss, J., Smit, R., Kinghorn, J.R., van den Hondel, C.A., Scazzocchio, C., 1995. The intergenic region between the divergently transcribed niiA and niaD genes of Aspergillus nidulans contains multiple NirA binding sites which act bidirectionally. Mol. Cell. Biol. 15, 5688–5699. https://doi.org/10.1128/MCB.15.10.5688

Samavarchi-Tehrani, P., Samson, R., Gingras, A.-C., 2020. Proximity Dependent Biotinylation: Key Enzymes and Adaptation to Proteomics Approaches *. Mol. Cell. Proteomics 19, 757–773. https://doi.org/10.1074/mcp.R120.001941

Schüller, A., Wolansky, L., Berger, H., Studt, L., Gacek-Matthews, A., Sulyok, M., Strauss, J., 2020. A novel fungal gene regulation system based on inducible VPR-dCas9 and nucleosome map-guided sgRNA positioning. Appl. Microbiol. Biotechnol. 104, 9801–9822. https://doi.org/10.1007/s00253-020-10900-9

Seo, J.-A., Yu, J.-H., 2006. The phosducin-like protein PhnA is required for Gbetagamma-mediated signaling for vegetative growth, developmental control, and toxin biosynthesis in Aspergillus nidulans. Eukaryot. Cell 5, 400–410. https://doi.org/10.1128/EC.5.2.400-410.2006

Singer-Krüger, B., Jansen, R.-P., 2022. Proteomic Mapping by APEX2-Catalyzed Proximity Labeling in Saccharomyces cerevisiae Semipermeabilized Cells. Methods Mol. Biol. Clifton NJ 2477, 261–274. https://doi.org/10.1007/978-1-0716-2257-5_15

Todd, R.B., Fraser, J.A., Wong, K.H., Davis, M.A., Hynes, M.J., 2005. Nuclear Accumulation of the GATA Factor AreA in Response to Complete Nitrogen Starvation by Regulation of Nuclear Export. Eukaryot. Cell 4, 1646–1653. https://doi.org/10.1128/EC.4.10.1646-1653.2005

Xiong, Z., Lo, H.P., McMahon, K.-A., Parton, R.G., Hall, T.E., 2021. Proximity Dependent Biotin Labelling in Zebrafish for Proteome and Interactome Profiling. Bio-Protoc. 11, e4178. https://doi.org/10.21769/BioProtoc.4178

Yang, X., Wen, Z., Zhang, D., Li, Z., Li, D., Nagalakshmi, U., Dinesh-Kumar, S.P., Zhang, Y., 2021. Proximity labeling: an emerging tool for probing in planta molecular interactions. Plant Commun. 2, 100137. https://doi.org/10.1016/j.xplc.2020.100137

Zhang, Y., Li, Y., Yang, X., Wen, Z., Nagalakshmi, U., Dinesh-Kumar, S.P., 2020. TurboID-Based Proximity Labeling for In Planta Identification of Protein-Protein Interaction Networks. J. Vis. Exp. JoVE. https://doi.org/10.3791/60728

Atanasoff-Kardjalieff, A. K., Studt, L., 2022. Secondary Metabolite Gene Regulation in Mycotoxigenic Fusarium Species: A Focus on Chromatin. Toxins. 14**,** 96.

Berger, H., et al., 2008. Dissecting individual steps of nitrogen transcription factor cooperation in the Aspergillus nidulans nitrate cluster. Mol Microbiol. 69**,** 1385-98.

Berger, H., et al., 2006. The GATA factor AreA regulates localization and in vivo binding site occupancy of the nitrate activator NirA. Mol Microbiol. 59**,** 433-46.

Bernreiter, A., et al., 2007. Nuclear export of the transcription factor NirA is a regulatory checkpoint for nitrate induction in Aspergillus nidulans. Molecular and Cellular Biology. 27**,** 791-802.

Boettcher, B., Barral, Y., 2013. The cell biology of open and closed mitosis. Nucleus. 4**,** 160-5.

Burger, G., et al., 1991. Molecular cloning and functional characterization of the pathway- specific regulatory gene nirA, which controls nitrate assimilation in Aspergillus nidulans. Mol Cell Biol. 11**,** 795-802.

Connolly, L. R., et al., 2013. The Fusarium graminearum histone H3 K27 methyltransferase KMT6 regulates development and expression of secondary metabolite gene clusters. PLoS genetics. 9**,** e1003916.

Cove, D. J., 1979. Genetic studies of nitrate assimilation in Aspergillus nidulans. Biol Rev Camb Philos Soc. 54**,** 291-327.

613 Davies, J. R., et al., 2004. Potential link between the NIMA mitotic kinase and nuclear membrane
614 fission during mitotic exit in Aspergillus nidulans. Eukaryot Cell. 3, 1433-44.
615 Deng, L., et al., 2013. Dissociation kinetics of the streptavidin-biotin interaction measured using
616 direct electrospray ionization mass spectrometry analysis. J Am Soc Mass Spectrom. 24, 49-
617 56.
618 Gacek-Matthews, A., et al., 2016. KdmB, a Jumonji Histone H3 Demethylase, Regulates Genome-
619 Wide H3K4 Trimethylation and Is Required for Normal Induction of Secondary Metabolism in
620 Aspergillus nidulans. PLoS genetics. 12, e1006222.
621 Gacek, A., Strauss, J., 2012. The chromatin code of fungal secondary metabolite gene clusters. Appl
622 Microbiol Biotechnol. 95, 1389-404.
623 Gallmetzer, A., et al., 2015. Reversible Oxidation of a Conserved Methionine in the Nuclear Export
624 Sequence Determines Subcellular Distribution and Activity of the Fungal Nitrate Regulator
625 NirA. PLoS Genetics. 11, e1005297.
626 Georgiou, X., et al., 2023. The interactome of the UapA transporter reveals putative new players in
627 anterograde membrane cargo trafficking. Fungal Genetics and Biology. 169, 103840.
628 Harris, S. D., et al., 2009. Morphology and development in Aspergillus nidulans: a complex puzzle.
629 Fungal Genet Biol. 46 Suppl 1, S82-S92.
630 Joseph, J. D., Means, A. R., 2000. Identification and characterization of two Ca2+/CaM-dependent
631 protein kinases required for normal nuclear division in Aspergillus nidulans. J Biol Chem. 275,
632 38230-8.
633 Karahoda, B., et al., 2022. The KdmB-EcoA-RpdA-SntB chromatin complex binds regulatory genes and
634 coordinates fungal development with mycotoxin synthesis. Nucleic Acids Research. 50, 9797-
635 9813.
636 Kudla, B., et al., 1990. The regulatory gene areA mediating nitrogen metabolite repression in
637 Aspergillus nidulans. Mutations affecting specificity of gene activation alter a loop residue of
638 a putative zinc finger. Embo J. 9, 1355-64.
639 Lamb, H. K., et al., 2003. The negative transcriptional regulator NmrA discriminates between oxidized
640 and reduced dinucleotides. The Journal of Biological Chemistry. 278, 32107-32114.
641 Langdon, T., et al., 1995. Mutational analysis reveals dispensability of the N-terminal region of the
642 Aspergillus transcription factor mediating nitrogen metabolite repression. Mol Microbiol. 17,
643 877-88.
644 Lemmon, M. A., 2004. Pleckstrin homology domains: not just for phosphoinositides. Biochem Soc
645 Trans. 32, 707-11.
646 Li, H., et al., 2021. Thiol-Cleavable Biotin for Chemical and Enzymatic Biotinylation and Its Application
647 to Mitochondrial TurboID Proteomics. J Am Soc Mass Spectrom. 32, 2358-2365.
648 May, D. G., et al., 2020. Comparative Application of BioID and TurboID for Protein-Proximity
649 Biotinylation. Cells. 9, 1070.
650 Muro-Pastor, M. I., et al., 1999. The GATA factor AreA is essential for chromatin remodelling in a
651 eukaryotic bidirectional promoter. Embo J. 18, 1584-97.
652 Muro-Pastor, M. I., et al., 2004. A paradoxical mutant GATA factor. Eukaryot Cell. 3, 393-405.
653 Pfannenstiel, B. T., Keller, N. P., 2019. On top of biosynthetic gene clusters: How epigenetic
654 machinery influences secondary metabolism in fungi. Biotechnol Adv. 37, 107345.
655 Punt, P. J., et al., 1995. The intergenic region between the divergently transcribed niiA and niaD
656 genes of Aspergillus nidulans contains multiple NirA binding sites which act bidirectionally.
657 Molecular and Cellular Biology. 15, 5688-5699.
658 Reyes-Dominguez, Y., et al., 2012. Heterochromatin influences the secondary metabolite profile in
659 the plant pathogen Fusarium graminearum. Fungal Genet Biol. 49, 39-47.
660 Scazzocchio, C., 2000. The fungal GATA factors. Curr Opin Microbiol. 3, 126-31.
661 Scazzocchio, C., Arst, H. N., Regulation of nitrate assimilation in Aspergillus nidulans. In: J. L. Wray, J.
662 R. Kinghorn, Eds.), Molecular and genetic aspects of nitrate assimilation. Oxford Science
663 Publications, Oxford, 1989, pp. 299-313.

664 Schinko, T., et al., 2010. Transcriptome analysis of nitrate assimilation in Aspergillus nidulans reveals
665 connections to nitric oxide metabolism. Mol Microbiol. 78, 720-38.
666 Sosa Ponce, M. L., et al., 2024. Lipids and chromatin: a tale of intriguing connections shaping genomic
667 landscapes. Trends Cell Biol.
668 Soyer, J. L., et al., 2014. Epigenetic control of effector gene expression in the plant pathogenic fungus
669 Leptosphaeria maculans. PLoS Genet. 10, e1004227.
670 Stammers, D. K., et al., 2001. The structure of the negative transcriptional regulator NmrA reveals a
671 structural superfamily which includes the short-chain dehydrogenase/reductases. Embo J.
672 20, 6619-26.
673 Strauss, J., et al., 1998. The regulator of nitrate assimilation in ascomycetes is a dimer which binds a
674 nonrepeated, asymmetrical sequence. Molecular and Cellular Biology. 18, 1339-1348.
675 Studt, L., et al., 2016. Knock-down of the methyltransferase Kmt6 relieves H3K27me3 and results in
676 induction of cryptic and otherwise silent secondary metabolite gene clusters in Fusarium
677 fujikuroi. Environmental microbiology. 18, 4037-4054.
678 Trinkle-Mulcahy, L., 2019. Recent advances in proximity-based labeling methods for interactome
679 mapping. F1000Res. 8.
680 Virag, A., Harris, S. D., 2006. Functional characterization of Aspergillus nidulans homologues of
681 Saccharomyces cerevisiae Spa2 and Bud6. Eukaryot Cell. 5, 881-95.
682 Wong, K. H., et al., 2007. Transcriptional control of nmrA by the bZIP transcription factor MeaB
683 reveals a new level of nitrogen regulation in Aspergillus nidulans. Mol Microbiol. 66, 534-51.
684 Yin, L. M., et al., 2020. Structural Characteristics, Binding Partners and Related Diseases of the
685 Calponin Homology (CH) Domain. Front Cell Dev Biol. 8, 342.

686

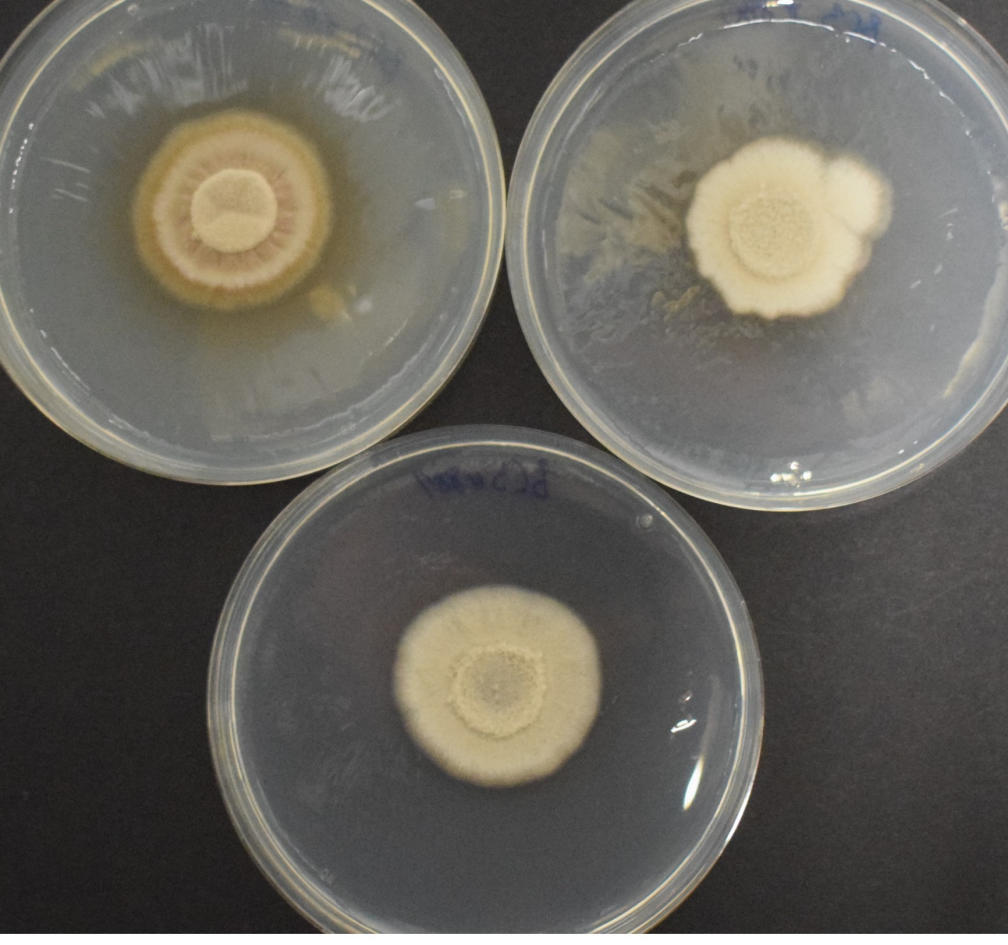

Supplementary Figure 1: Phenotypic appearance of the tested strains; AreA-HA (top, left), CasID-sgRNA (top, right), CasID + sgRNA (bottom)

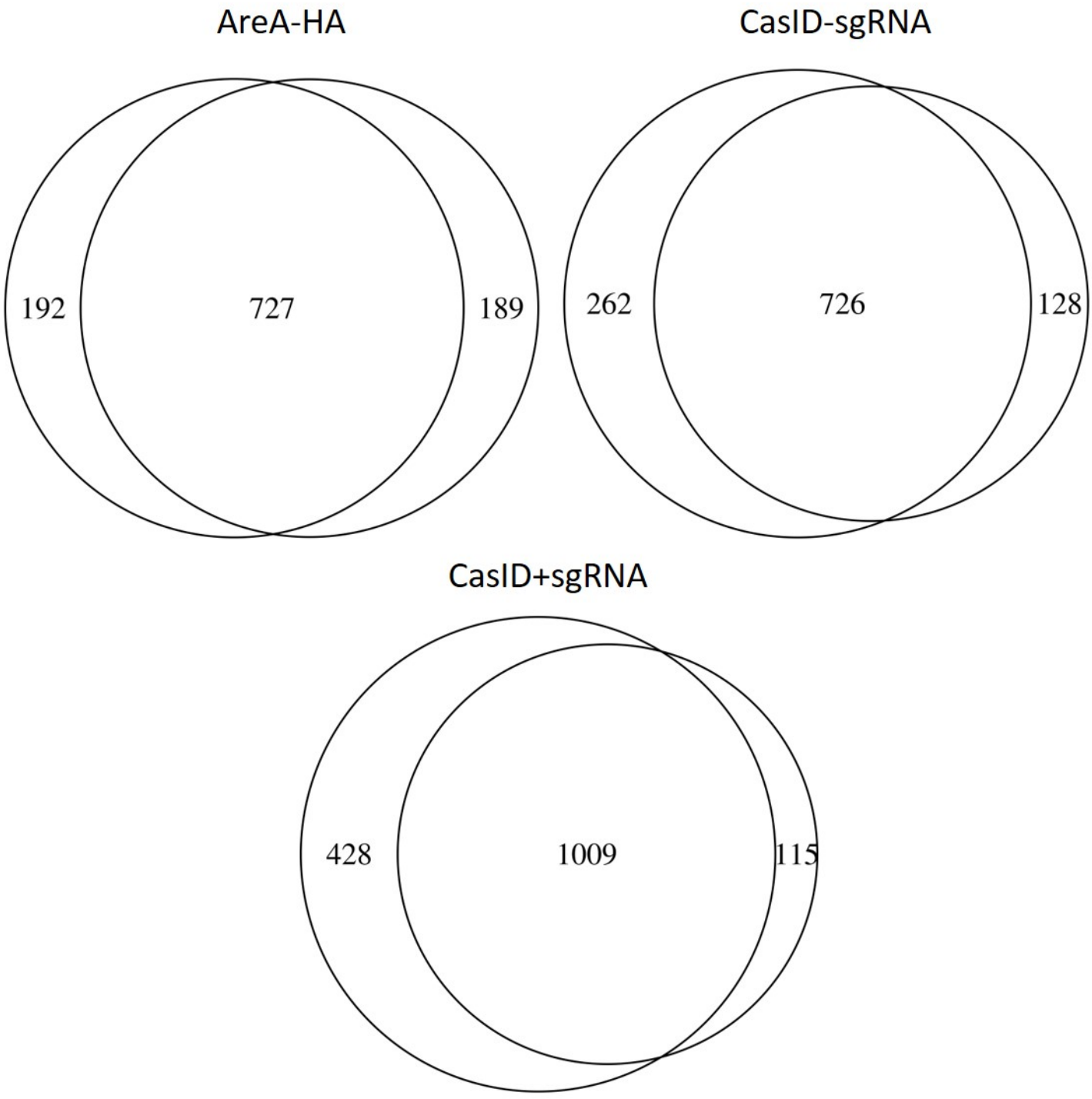
AreA-HA
192
727
189
CasID-sgRNA
262
726
128
CasID+sgRNA
428
1009
115